

Phase separation in two-dimensional electron systems: Experimental view

V. M. Pudalov¹

¹*V. L. Ginzburg Research Center at P. N. Lebedev Physical Institute, Moscow 119991, Russia.
HSE University, Moscow 101000, Russia*

Key experimental results on unveiling and studying properties of a multiphase state that arises in two-dimensional electron systems due to the interplay of interelectron interactions and disorder are reviewed. We focus on the experimental results obtained with high mobility Si- field effects structures (Si-MOS), in which the interaction effects at low carrier concentrations are most pronounced due to the strong e-e interactions, multi-valley spectrum, and the short-range character of the random potential. The reviewed effects of phase separation include features in transport, magnetotransport and thermodynamics. Consideration of a number of experimental results is supplemented with a brief review of their theoretical interpretation.

CONTENTS

I. Introduction	1
II. Two-dimensional electron systems with strong interactions. Theory overview	1
A. Negative compressibility and phase separation. Analytical results	2
B. Taking disorder into account	2
1. Results in the framework of quantum interaction corrections and renormalization group theory	2
2. Numerical results	2
3. Non-linear screening approach. Numerical modelling	3
III. Compressibility of 2DE systems: Experimental studies	4
A. Earlier capacitance measurements	4
B. Field penetration measurements	5
C. Local compressibility measurements	6
IV. Phase separation effects revealed in thermodynamics and transport	7
A. Evidence of the “spin-droplet” state in thermodynamic spin magnetization	7
B. Phase separation effects in charge transport	7
1. Magnetotransport in the in-plane field	8
2. Phase separation effects in oscillatory magnetotransport	9
3. Phase separation effects in zero field transport	10
C. Phase separation effect in spin susceptibility	11
V. Conclusions	12
VI. Acknowledgements	13
References	13

I. INTRODUCTION

Recently, phase separation effects came to the fore as the objects of intense attention in condensed matter physics. Historically first and the most remarkable phase separation effects were found in manganites [1], then the phase separation appeared to play an essential role in high-Tc superconductors [2, 3], low-dimensional organic crystals [4], etc. To date it became clear that phase separation is ubiquitous rather than exotic.

Several comprehensive reviews were published in recent years [5, 6], they considered mainly theoretical aspects of the physics of phase separation. The current mini-review partially compensates this shortcoming and considers several representative manifestations of the phase separation in experiments with two-dimensional (2D) systems of interacting electrons. In all considered examples the driving force behind the phase separation is the competition between disorder and interparticle interactions. It is known that the effects of interaction are the stronger, the lower the dimension of the system.

II. TWO-DIMENSIONAL ELECTRON SYSTEMS WITH STRONG INTERACTIONS. THEORY OVERVIEW

Correlation plays a crucial role for electrons with a $1/r$ pair potential moving in a neutralizing charge background [7]. Its importance grows both with lowering the density and the space dimensionality, and tends to qualitatively change the predictions of simple schemes, such as the Hartree-Fock HF or random-phase approximation RPA [7]. The interaction strength is commonly characterized by the dimensionless parameter r_s - the ratio of the potential interaction energy E_{ee} and kinetic Fermi energies E_F ; for electrons in (001)-Si MOS structure $r_s = 2.63 \times (10^{12}/n[\text{cm}^{-2}])^{1/2}$ [8].

In the low-density strongly correlated electron liquid, the energy balance determining the system properties is played on a very minute scale and, to get meaningful predictions, a great accuracy such as the one afforded by quantum Monte Carlo (QMC) methods is necessary [7].

In two dimensional systems, the interplay of disorder and electron-electron interactions gives birth to many exciting effects, some of them are considered below. We begin with the negative compressibility of the electron liquid - the effect that paves the way for phase separation.

A. Negative compressibility and phase separation. Analytical results

The inverse compressibility (or $\partial\mu/\partial n$) of a system reflects how its electrochemical potential changes with carrier density

$$\kappa^{-1} = n^2 \frac{\partial^2 E_{tot}}{\partial n^2} = n^2 \left(\frac{\partial\mu}{\partial n} \right), \quad (1)$$

with n being the carrier density, and μ the electrochemical potential. For noninteracting electrons κ is proportional to the single-particle density of states D , which in 2DE systems is density independent, being $D_2 = g_v m / (\pi \hbar^2)$, where g_v - is the valley degeneracy ($g_v = 2$ for (001)-Si MOS).

This picture, however, changes drastically when interactions are included. It was realized already in the 1980s that compressibility of the 2DES can become negative at low densities, owing to electron-electron interactions [9]. Exchange and correlation effects weaken the repulsion between electrons, thereby reducing the energy cost, thus leading to negative and singular corrections to $\partial\mu/\partial n$. At zero magnetic field this effect is due primarily to the exchange energy while at high field the correlation energy plays a significant role as well [10].

Within the Hartree-Fock (HF) theory, which includes both the density-of-states and exchange terms, for a clean system with no disorder one gets:

$$\frac{\partial\mu}{\partial n} = \frac{\pi \hbar^2}{m} - \left(\frac{2}{\pi} \right)^{1/2} \frac{e^2}{4\pi\epsilon} \frac{1}{n^{1/2}} \quad (2)$$

Thus, upon decreasing density, the compressibility for a clean system gets negative and tends to $-\infty$. The sign change of compressibility means that when the concentration of electrons in the system varies, the changes in the potential energy due to the interelectron interaction, having the opposite sign, exceed the changes in the kinetic energy. Experimentally, the sign change of $(\partial\mu/\partial n)^{-1}$ has been found first in the capacitance and chemical potential measurements in magnetic field [11–13] and later was confirmed in the measurements performed by the field penetration technique in zero field [14–16] (Sec. III B).

B. Taking disorder into account

Disorder is inevitably present in real two-dimensional systems [17]. No matter how small the potential fluctuations in the most advanced 2D structures are, they

lead to a significant change in the behavior of thermodynamics and transport in the system as carrier density decreases.

1. Results in the framework of quantum interaction corrections and renormalization group theory

Explicit calculations on the “metallic” side (high conductivity $\sigma \times (h/e^2) = E_F \tau / \hbar \gg 1$), within the renorm-group and interaction correction theory, show no singular correction to the compressibility in leading order in disorder [18–22], and even to the second order [23].

There were several pioneering efforts [24, 25] in addressing the interplay between interaction and disorder and their effect in thermodynamic properties, by calculating corrections to the compressibility from the exchange and correlation contribution to the ground state energy [24]. However, the predicted vanishing of the compressibility as the transition to the localized state is approached from the metallic side is at odd with experimental results (Section III).

2. Numerical results

The unlimited divergency of κ^{-1} for the clean 2DE system is cut-off in the presence of disorder. Having obtained the equation of state [i.e., $E(r_s)$] of the normal liquid, Tanatar and Ceperley [26] calculated the compressibility using

$$\frac{\kappa_0}{\kappa} = 1 - \frac{\sqrt{2} r_s}{\pi} + \frac{r_s^4}{8} \left[\frac{d^2}{dr_s^2} - \frac{1}{r_s} \frac{d}{dr_s} \right] E_c. \quad (3)$$

Here $\kappa_0 = \pi r_s^4 / 2$ is the compressibility of a noninteracting system (see Fig. 1a), and E_c - correlation energy [26] In the above equation, the compressibility becomes negative around $r_s = 2.03$, slightly before the Hartree-Fock result of 2.22.

Within the self-consistent HF approximation and the deformable jellium model, Orozco et al. [27] calculated the ground-state compressibility of the 2DE system for the density region which includes the liquid to localized phase transition. A sudden change in the behavior of the chemical potential and a large divergence in the inverse compressibility have been found for low densities. The change of sign of the inverse compressibility and its overall behavior versus r_s calculated in this work, agree qualitatively with the behavior of κ^{-1} observed in experiments (see Section III).

The thermodynamic compressibility can be readily calculated from the ground-state energy

$$\frac{\kappa_0}{\kappa} = -\frac{r_s^3}{8} \left[\frac{\partial E_g}{\partial r_s} - r_s \frac{\partial^2 E_g}{\partial r_s^2} \right]. \quad (4)$$

Asgari and Tanatar [28] calculated the ground state energy and compressibility within DFT and dynamical

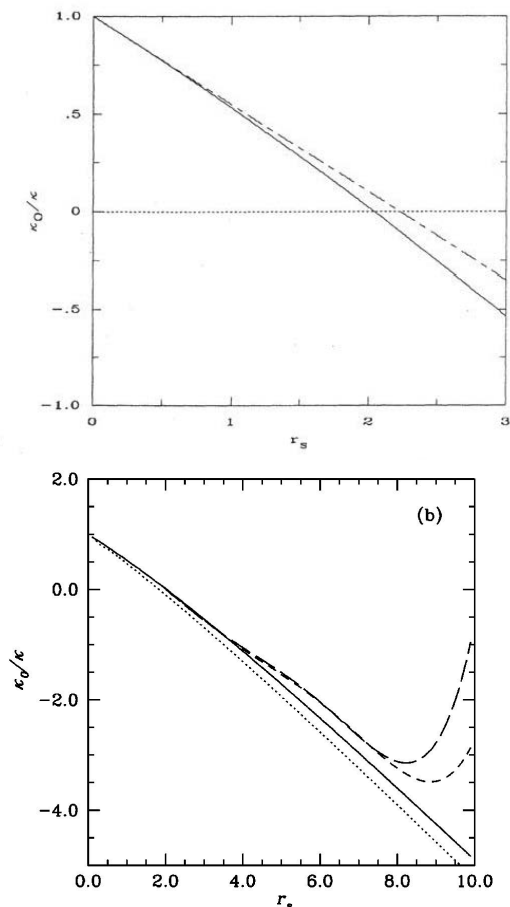


FIG. 1. (a) Inverse compressibility κ_0/κ of the electron gas as function of density parameter r_s calculated using Eq. (3). Dashed line is the compressibility in the Hartree-Fock approximation. Adapted from Ref. [26]. (b) κ_0/κ calculated for a wider range of r_s . The short and long-dashed curves are for impurity densities $n_i = 5 \times 10^{10}$ and 10^{11}cm^{-2} , respectively. Adapted from Ref. [28].)

mean field formulation. The results are presented in Fig. 1b. The solid curve here shows κ^{-1} for a clean system. They considered the disorder effect within two models: (i) a density independent scattering rate γ - similar to Si and Varma [24], and (ii) in the mode coupling approximation, with γ dependent on r_s through the screened impurity scattering potential. The dotted curve was calculated with a constant γ . It stays negative at low density, qualitatively similar to that for the clean system. Most important, κ_0/κ calculated within the mode-coupling approximation, which includes the screened electron-impurity scattering potential, exhibits a minimum and starts rising towards positive values. Thus, the inverse compressibility upturn at low densities is the effect of disorder solely. On the other hand, the disorder does not affect κ in the range of $r_s = 2 \div 4$.

The density at which the calculated inverse compressibility experiences a minimum, depends on the impurity

density n_i (see Fig. 1b). In experiments [29–31] the inverse compressibility also shows an upturn after going through a minimum. Initially [29], this minimum has been suggested as a thermodynamic signature of the metal-insulator transition. However, later on the two effects were disentangled and the anomalous behavior of $1/\kappa$ was attributed to the inhomogeneous nature of the insulating phase, as demonstrated experimentally [30–32] and theoretically [27, 28, 33, 34]. Thus, the calculations Ref. [28] yield the overall $1/\kappa(r_s)$ dependence similar to that observed in the experiments (Section III B).

3. Non-linear screening approach. Numerical modelling

Shi and Xie [33] investigated spatial distribution of carrier density and the compressibility of 2D electron systems by using the local density approximation. A slowly varied disorder potential was applied to simulate the disorder effect. To investigate the density distribution of a disordered 2D electron system, within DFT, the total electron energy was calculated as

$$E(n) = E_T(n) + E_{ee}(n) + E_d(n) + E_x(n) + E_c(n) \quad (5)$$

Here $E_T(n)$ is the functional of the kinetic energy, $E_{ee}(n)$ is the direct Coulomb energy due to charge inhomogeneity, $E_d(n)$ is the disorder potential energy, $E_x(n)$, and $E_c(n)$ are the exchange and correlation energy, respectively. The ground state spatial density distribution was obtained by minimizing the total energy functional with respect to the density. A slowly varied disorder potential was applied to simulate the disorder effect. Shi and Xie found that at low average densities electrons form a droplet state which is a coexistence phase of high- and low-density regions. In calculating total exchange and correlation energy they used interpolated Tanatar and Ceperley QMC results for exchange and correlation energy density for the homogeneous 2DE system [26].

It was found that the compressibility anomaly observed in 2D systems which accompanies the metal-insulator transition can be attributed to the formation of the droplet state due to a disorder effect at low carrier densities. Figure 2 shows the density distribution of the system. It can be clearly seen that the electrons form some high density regions, while the density of other regions is essentially zero. Depending on the average density of the system, the high-density regions may connect to each other ($r_s = 10$), or form some isolated regions ($r_s = 19$). There exists a certain density $r_s = 14$, where the connectivity of the high-density regions changes (a percolation transition).

The e-e interaction is important for the conduction behavior of a dilute electron system in the sense that it makes the density distribution more extended because of the Coulomb repulsion. Figure 3 shows the density distribution for the free electron gas with the same density as in Fig. 2 by turning off the electron-electron interaction. The system forms only some isolated high density regions

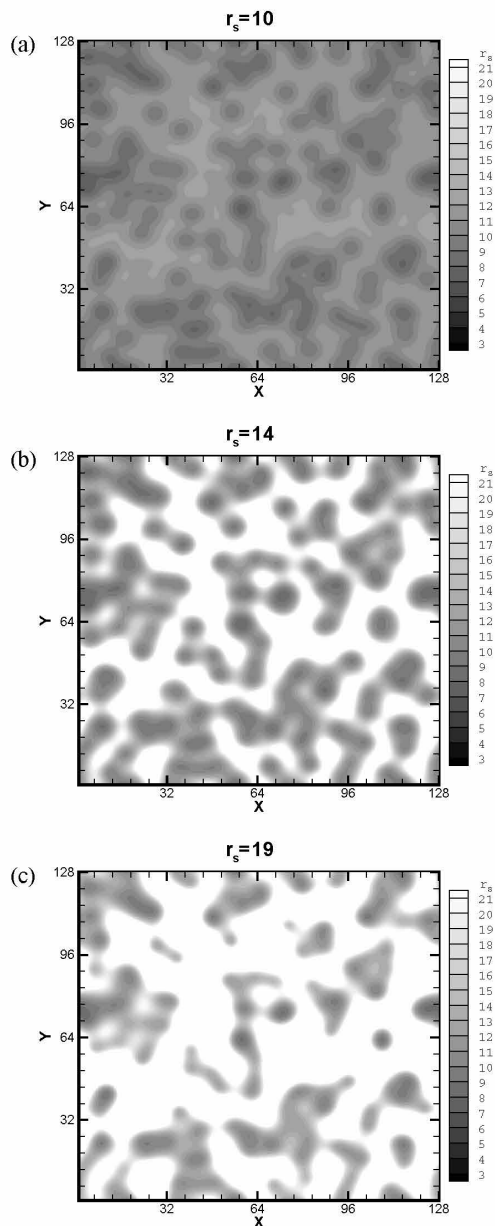


FIG. 2. Spatial density distributions for various average densities. The contour plot shows local density parameter $r_s = 1/\sqrt{\pi n}$. The density in the white area decreases rapidly to zero. The size of the system is set as $L = 256a_B^*$. The disorder potential is generated by off-plane charge impurities with $d = 10a_B^*$, $n_i = 2.5 \times 10^{-3}/(a_B^*)^2$. Adapted from Ref. [33].

at the most disordered areas, while the density distribution of the corresponding interacting system (Fig. 2b) is quite extensive at the same density. In other words, at a given disorder strength, the critical density for the free electron gas is much higher than for its interacting analogue.

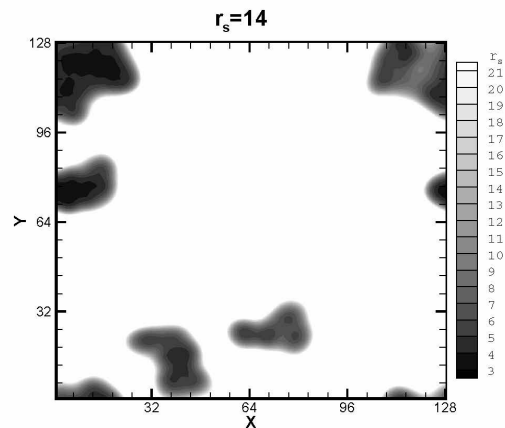


FIG. 3. Spatial density distribution for the free electron gas on the same disorder landscape as Fig. 2 at density $r_s = 14$. Adapted from Ref. [33]

III. COMPRESSIBILITY OF 2DE SYSTEMS: EXPERIMENTAL STUDIES

A. Earlier capacitance measurements

In earlier experiments [11–13, 35, 36], information about compressibility (or inverse density of states) was obtained from either capacitance measurements or from measurements of the electrochemical potential variations versus density in quantizing magnetic field. In the former case, the capacitance was measured by AC-bridge in the frequency range 6–75 Hz. The measured capacitance C is considered to be a series connection of the geometric and “quantum” parts:

$$C^{-1} = C_0^{-1} + e^2 S \left(\frac{\partial n}{\partial \mu} \right)^{-1}, \quad (6)$$

where C_0 is the capacitance in the $\partial \mu / \partial n \rightarrow 0$ limit which does not depend on B , and S is the 2DE layer area. C_0 may be estimated as follows:

$$C_0^{-1} = C^{-1}|_{B=0} - (e^2 S D_0)^{-1},$$

where the density of states $D_0 = \partial n / \partial \mu|_{B=0} = 8.37 \times 10^{14} (m^*/m_e) \text{cm}^{-2} \text{eV}^{-1}$ [8]. In order to separate the second “quantum” part from the geometric capacitance, the data taken in zero field was subtracted from that in magnetic field. Correspondingly, the zero field behavior of the compressibility remained inaccessible.

Figure 4 represents the difference $\Delta C(n)$ of the two dependences $\Delta C = -(C - C|_{B=0})$ measured with Si-MOSFET sample as a function of carrier density at three temperatures and in a fixed magnetic field of 11.7 Tesla. The measured difference equals to

$$\Delta C \approx (C^2 / e^2 S) [(\partial n / \partial \mu)^{-1} - D_0^{-1}]$$

The obtained dependence at $T = 4.2 \text{K}$ agrees with earlier capacitance measurements [37–39]. In particular,

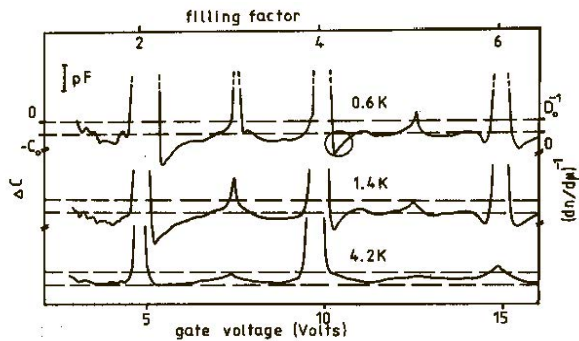


FIG. 4. ΔC dependences on V_g (proportional to the carrier density) for three temperatures and at field 11.7 Tesla. The upper horizontal axis shows the Landau level filling factors. Adapted from Ref. [11]

the $(\partial n/\partial \mu)^{-1}$ values at half-integer fillings are less than D_0^{-1} but positive. However, lowering the temperature to 1.4 K and to 0.6 K leads to the appearance of regions of filling factors where $(\partial n/\partial \mu)^{-1}$ gets negative. The appearance of these dips in the vicinity but somewhat away of the integer filling factors was exactly the feature predicted by Efros [10]. Indeed, in his language, the total electron energy acquires a term E_{ee} in addition to the single-particle term E_{1p} . Therefore, the inverse total density of states may be written as

$$D^{-1} = D_{1p}^{-1} + G_{ee}^{-1}.$$

G_{ee} was evaluated by Efros [10] as follows:

$$\begin{aligned} G_{ee} &= -(e^2 \alpha / \varepsilon) (\{\nu\} n_B)^{3/2}, & \{\nu\} \leq \frac{1}{2}, \\ &= -(e^2 \alpha / \varepsilon) \left[(1 - \{\nu\}) n_0^{3/2} \right], & \{\nu\} \geq \frac{1}{2}, \end{aligned}$$

where $\nu = n/n_B$ is the Landau levels filling factor, $n_B = 1/(2\pi l_B^2)$ – the Landau level degeneracy, $\{\nu\}$ – fractional part of the filling factor $\{\nu\} = \nu - \text{int}(\nu)$, and α is a dimensionless constant ($= 2$ for the classical Coulomb interaction).

The inverse thermodynamic density of states, correspondingly, is equal to [10]:

$$\begin{aligned} D_{ee}^{-1} &= - \left(\frac{3\alpha e^2}{4\pi\varepsilon} \right) (\{\nu\} n_B)^{-1/2}, & \{\nu\} \leq \frac{1}{2}, \\ &= - \left(\frac{3\alpha e^2}{4\pi\varepsilon} \right) [(1 - \{\nu\}) n_B]^{-1/2}, & \{\nu\} > \frac{1}{2} \end{aligned} \quad (7)$$

The negative compressibility signals a tendency of the 2DE system to break the homogeneous state. On the other hand, the stability of the entire 2D system with a negative compressibility is achieved in physical systems by the neutralizing background. For the gated 2D system, the stability condition was analyzed in Ref.[40].

B. Field penetration measurements

In the conventional capacitance technique, the capacitance between the 2D gas and a metal gate electrode is measured. The dominance of a large geometric term in the measured capacitance essentially forces one to vary some other parameter, like magnetic field [11–13, 36], temperature [41, 42], etc., and then subtract off a large, and constant, offset in order to uncover the quantum term. There are three major drawbacks to this technique. First, the geometric term is usually not accurately known and therefore the subtraction is uncertain. The geometric term produces a second difficulty as well: it may not actually remain constant as the external parameter, e.g. magnetic field is changed. Thirdly, the slowly-decaying eddy currents excited in 2DE system by ac-modulation of the carrier density [43] impede capacitance measurements at low temperatures in quantizing magnetic field.

The “floating gate” technique elaborated in Ref. [44] does not require field or density modulation and therefore can be used for electrochemical potential measurements even in the QHE regime [45, 46].

The alternative field penetration technique introduced by Eisenstein [14, 15] provides automatically subtracting the geometric term. This is achieved by use of a double layer 2D system and measuring the fraction of the ac electric field δE_0 which penetrates one layer and is detected by the second. The inset to Fig. 5 shows a schematic setup. The ac field δE_p penetrates through the upper layer and causes current flow through the external impedance Z , thus generating a detectable voltage V_{sig} .

Lower part of Fig. 5 shows a trace of the measured ac-current (proportional to penetration field) as a function of the gate voltage or electron density of the upper 2D layer. The penetration field measures the screening ability of the electrons which is inversely proportional to κ . The main advantage of this experimental approach is that it provides direct access to $\partial \mu / \partial N$ for the top 2DE layer without any offset signals (related with geometric capacitance contribution). Dultz and Jiang [29] have extended the field penetration method to a more conventional heterostructure with only a single layer of carriers.

Were the 2DE system noninteracting, the penetration to the bottom layer would be a few percent and would be positive. This result is qualitatively altered by e-e interactions that make the observed differential penetration negative. The minimum in the inverse compressibility was already detected in the measurements by Eisenstein [15].

This minimum attracted much interest when Dultz and Jiang [29] reported that in some samples the minimum virtually coincides with the metal-insulator transition in transport. They found [29] that the negative $1/\kappa$ at low densities reaches a minimum value at a certain density, and then increases dramatically with further decreasing n . This coincidence was initially considered as a thermodynamic signature of an interaction-driven

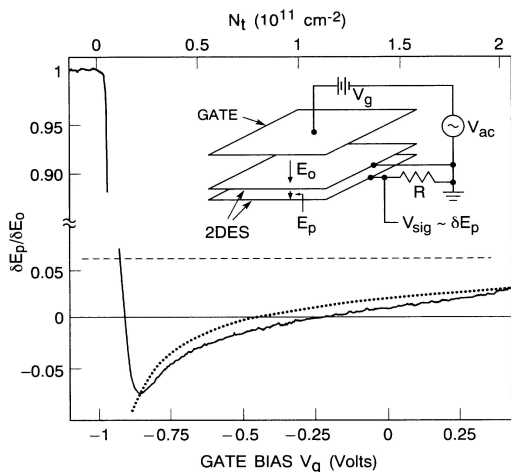


FIG. 5. Normalized penetrating field $\delta E_p/\delta E_0$ versus gate voltage at zero magnetic field and $T = 1.2\text{K}$. Dotted curve is calculated using Tanatar and Ceperley’s compressibility [26]. Upper axis gives carrier density of the top 2DE system. Dashed horizontal line - noninteracting case. Inset - experimental set-up. Adapted from Ref. [14].

phase transition [24, 47]. However, later on Allison et al. [32] measured simultaneously the compressibility, capacitance and resistivity in the vicinity of the metal-insulator transition with different samples. It was shown that the coincidence of the two effects in some samples, the inverse compressibility minimum and the sign change in transport $d\rho/dT$, is accidental.

C. Local compressibility measurements

Ilani et al. [30, 31] have performed local study of $\partial\mu/\partial n$ and expanded them into the low density regime, across transition to the localized state. Their measurements utilized single electron transistors (SET), located directly above a two-dimensional hole gas (2DHG) of inverted back-gated GaAs/AlGaAs structures. This technique allowed to probe the local behavior of $\partial\mu/\partial n$ as well as its spatial variations. At equilibrium, the Fermi energy is constant across the sample, and therefore a change in $\mu(n)$ induces a change in the electrostatic potential, which is readily deduced by measuring the change in current through the SET. The spatial resolution, determined from the size of the SET and its distance from the 2DHG, is $0.1 \times 0.5 \mu\text{m}^2$.

Instead of the anticipated monotonic dependence, local $\mu(n)$ exhibits a rich structure of oscillations. In the high density “metallic” regime, Ilani et al. observed long sawtooth oscillations. Superimposed on them and starting in close proximity to the onset of the localized state, a new set of rapid oscillations emerges (Fig. 6b). Their typical period is an order of magnitude smaller, and the amplitude grows continuously from the point of appearance to lower densities. All the oscillations, including

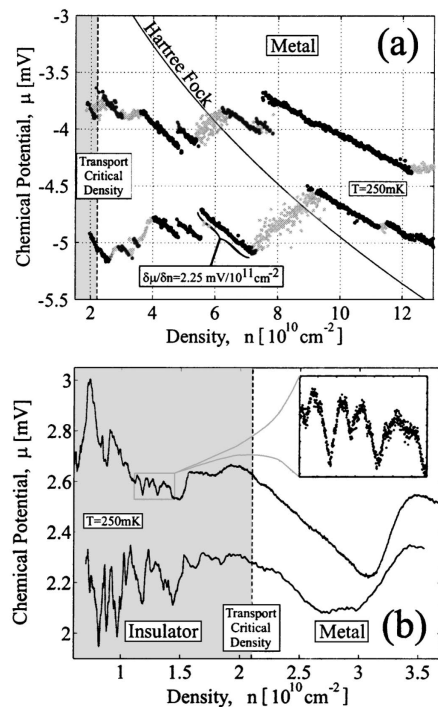


FIG. 6. (a) Measured $\mu(n)$ in the metallic regime (dots) together with the HF theory [Eq. (1)] for a clean system (solid line). The measured negative slopes are highlighted (dark symbols) to demonstrate their resemblance to the HF model. (b) Measured $\mu(n)$ across the MIT and in the insulating region. Inset: A closer look at the data in the insulating regime. Each slope is composed of many data points allowing an accurate determination of the slopes. Adapted from Ref.[30]

the fine structure seen on the left side of Fig. 6b, were reproducible and did not exhibit hysteresis or sweep rate dependence.

The sawtooth profile is reminiscent of the electrochemical potential behavior for a quantum dot as a function of the number of electrons [48] and, hence, suggests the existence of discrete charging events. Thus, the measured μ of the 2DHG varies undisturbed along the segments with negative slopes, until a certain bias between the 2DHG and the SET makes recharging of an intermediate localized state energetically favorable. This causes a sharp drop in the electrostatic potential, after which μ continues to vary smoothly until the next screening event occurs.

Ilani et al. reconstructed the basic $\mu(n)$ dependence by assembling the undisturbed segments together; the results are shown in Fig. 7, for five different SETs placed apart from each other. In the “metallic” regime (high density) all the data collapse onto a single curve in Fig. 7, rather close to the HF model prediction.

In the insulating phase, assuming that the new set of oscillations is caused by the same mechanism (screening by traps), the authors extracted the slopes and added them to the same plot of $\partial\mu/\partial n$ (see Fig. 7). Unlike in

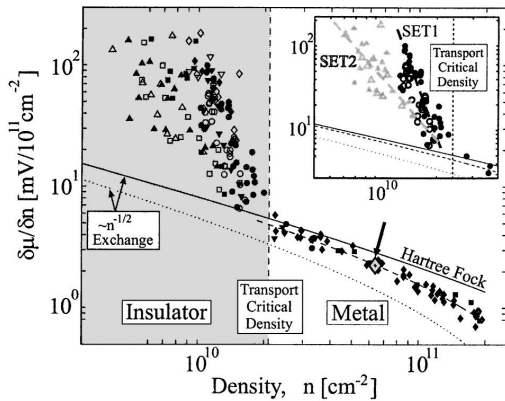


FIG. 7. $|d\mu/dn|$ collected from several SETs on several samples. In the insulating regime, the $|d\mu/dn|$ magnitude includes both negative and positive slopes. Each point corresponds to a well-defined segment in the $\mu(n)$ trace. The point marked by an arrow corresponds to the marked segment in Fig. 6a. Inset: Results from two SETs on the same device demonstrating the spatial dependence of $|d\mu/dn|$ in the insulating side. Adapted from Ref. [30]

the metallic phase where the system clearly has a negative $\partial\mu/\partial n$, in the insulating phase the sign of the compressibility is not known a priori. Therefore, in Fig. 7 the absolute value is shown of both negative and positive slopes, all of which deviate considerably from the expected $n^{-1/2}$ power law. The deviation becomes greater than an order of magnitude at the lowest density and indicates a change in the screening properties of the 2DHG at the transition to the localized state. The fluctuations in the slopes, observed on the insulating side, are reproducible and suggest that mesoscopic effects are present. Furthermore, the average behavior of $\partial\mu/\partial n$ in this fluctuating regime is position dependent (see the inset in Fig. 7). Such dependence on position indicates that once the system crosses into the insulating phase it becomes spatially inhomogeneous.

The local measurements [31] emphasize the important role of charged traps in the ground state thermodynamics of the 2D system. It might have a direct relationship to the models where the 2D gas and charge traps coexist in equilibrium, particularly [49, 50]. To summarize shortly the results of local measurements [30], it was found that the behavior of $\partial\mu/\partial n$ in the metallic phase on average follows the HF model suggesting the 2D system to be almost spatially homogeneous. In contrast, the insulating phase is found to be spatially inhomogeneous.

IV. PHASE SEPARATION EFFECTS REVEALED IN THERMODYNAMICS AND TRANSPORT

A. Evidence of the “spin-droplet” state in thermodynamic spin magnetization

The method of $\partial\mu/\partial B$ thermodynamic measurements was introduced and substantiated in Refs. [51, 52]. To probe purely spin susceptibility, free of orbital contribution, measurements in Refs. [51, 52] were performed in magnetic field B_{\parallel} aligned strictly parallel to the 2D plane. In this technique, the applied magnetic field is modulated with a small amplitude δB and the excited recharging current of the Si-MOS structure [52] is measured: $\delta I = [i\omega C_0 \delta B / e](\partial\mu/\partial B)$. Here C_0 is the known capacitance of the “gate - 2D layer” structure. From the measured recharging current the quantity $\partial\mu/\partial B$ is found and, due to the Maxwell relation, directly yields the magnetization per electron $\partial M/\partial n$.

In order to explore interaction effects the measurements in [53] were performed in weak fields less than temperature, $g\mu_B B \leq k_B T$. In Figure 8 one can see that at low densities $\partial M/\partial n$ becomes positive and in all cases is much greater than expected for the Pauli spin susceptibility. When the field increases (while still being smaller than the temperature, $g\mu_B B < k_B T$), $\partial M/\partial n$ sharply increases and exceeds the Bohr magneton by more than a factor of two at low temperatures (Fig. 8). Such behavior of $\partial M/\partial n$ is reminiscent of the dependence anticipated for free spins [53]. However, the fact that $\partial M/\partial n$ exceeds the Bohr magneton points to a ferromagnetic ordering of the electron spins. The magnetization curves $\partial M/\partial n$ (Fig. 8) saturate in the field $b = \mu_B B / (k_B T) \sim 0.25$, signaling that the particles which respond to the field modulation have spins $1/(2b) \approx 2$, rather than $1/2$. This result is the “smoking-gun-evidence” of the emergence of a two-phase state in the 2D system consisting of a paramagnetic Fermi liquid and ferromagnetic domains (called “spin droplets”) with the total spin ~ 2 , comprising, respectively, four or more electrons.

The existence of the two-phase state is not a unique property of the low-density state solely, the spin droplets were detected in Ref. [53] in the wide range of densities, up to $n \approx 2 \times 10^{11} \text{cm}^{-2}$ that is twice the critical density of the onset of the insulating state, i.e. in the regime of high metallic metallic conduction $\sigma \approx 80e^2/h$.

B. Phase separation effects in charge transport

In Ref. [54], several features have been revealed in magnetotransport, zero-field transport, and thermodynamic spin magnetization for a 2D correlated electron system. These features have been associated with the two-phase state. More specifically:

(i) in magnetoconductivity the novel regime of magnetoconductance sets above a density-dependent temperature

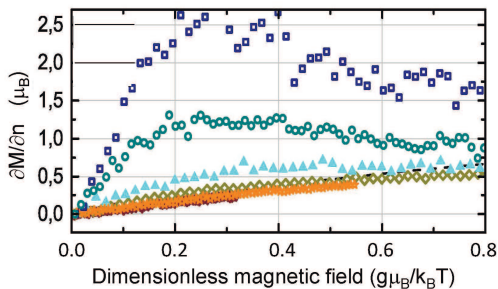


FIG. 8. Magnetization per electron $\partial M/\partial n$ in weak field plotted versus the normalized magnetic field for a carrier density of $5 \times 10^{10} \text{ cm}^{-2}$ at several temperatures ($T = 0.8, 1.2, 1.8, 4.2, 7, 10, 24 \text{ K}$, from top down). Adapted from Ref. [53]

$T_{\text{kink}}(n)$.

(ii) In the temperature dependence of zero-field resistivity an inflection point is observed at about the same temperature $T_{\text{infl}}(n) \approx T^*$.

(iii) In thermodynamic magnetization the weak-field spin susceptibility per electron, $\partial\chi/\partial n \equiv \partial^2 M/\partial n$ changes sign at $T_{dM/dn}(n) \approx T^*$.

All three notable temperatures, T_{kink} , T_{infl} , and $T_{dM/dn}$ are close to each other (see Fig. 9), and are intrinsic to strongly correlated regime solely. It is shown below that these features can be described within the framework of the phase separation approach.

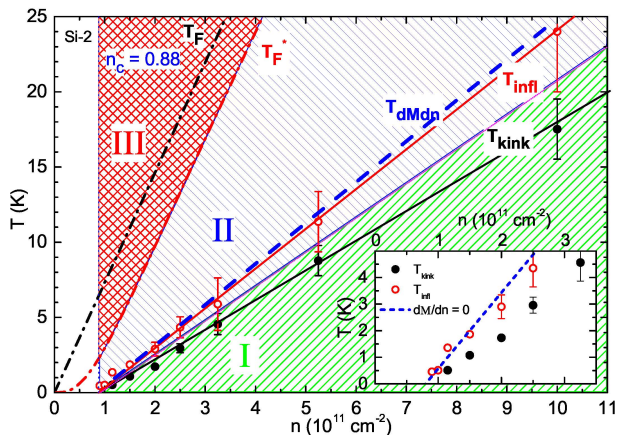


FIG. 9. Empirical phase diagram of the 2DE system. Dashed areas are (I) the ballistic interaction regime and (II) the anomalous magnetoconductance regime. Hatched area (III) is the nondegenerate regime, the blank area at $n < n_c$ is the localized phase. Full dots: the kink temperature T_{kink} ; open dots: the inflection point T_{infl} . Dash-dotted curves show the calculated bare (T_F) and the renormalized (T_F^*) Fermi temperatures. The insert blows up the low-density region; the dashed line is $T_{dM/dn}$ [54]. Adapted from [54].

1. Magnetotransport in the in-plane field

Regarding the zero field transport and magnetotransport, their features require more detailed explanation.

In the conventional theory of interaction corrections (IC) [55], the lowest order variations of the magnetoconductivity (MC) with weak in-plane field $g\mu_B B < k_B T \ll k_B T_F$ at a fixed temperature T are parabolic. This is clear from symmetry arguments, and also follows from the IC theory and the screening theory [56, 57].

$$\sigma = \sigma_0 - a_\sigma B^2 + \mathcal{O}(B^2); \quad \rho = \rho_0 + a_\rho B^2 + \mathcal{O}(B^2), \quad (8)$$

where by definition

$$a_\sigma \equiv -\frac{1}{2} \frac{\partial^2 \sigma}{\partial B^2} \Big|_{B=0} = \frac{1}{2\rho^2} \frac{\partial^2 \rho}{\partial B^2}; \quad a_\rho \equiv \frac{1}{2} \frac{\partial^2 \rho}{\partial B^2} \Big|_{B=0}.$$

In Ref. [54] the in-plane field MC was studied in detail and quantified in terms of the prefactor $a_\sigma(T, n)$. Within the IC theory, the $\sigma(T, B)$ variation in the 2DE system is described by the sum of the interference correction and e-e interaction corrections [55, 58]

$$\Delta\sigma(T) \approx \Delta\sigma_C(T, B) + n_T(B)\Delta\sigma_T(T, B) + \mathcal{O}\left(\frac{1}{k_F l}\right).$$

Here the first term combines single-particle interference and interaction corrections in the singlet channel, and the second term is the interaction corrections in the triplet channels, $k_F l \gg 1$ is the dimensionless conductivity. Within the same approach, MC in the weak in-plane field originates from the field dependence of the effective number of triplet channels $n_T(B)$, that in its turn is due to the Zeeman splitting [55].

As a result, the first order interaction corrections to MC in the diffusive and ballistic interaction regime $\Delta\sigma \equiv \sigma(T, B) - \sigma(T, 0)$ may be written in terms of a_σ as follows [55]:

$$a_\sigma(T) \propto \begin{cases} (1/T)^2, & T\tau \ll 1 \\ (1/T), & T\tau \gg 1. \end{cases} \quad (9)$$

Their explicit expressions are given in Ref. [55].

Thus, according to the IC theory predictions, as temperature *increases*, the MC should cross over from $(1/T^2)$ to $(1/T)$ temperature dependence. This theory prediction is confirmed in measurements with low-mobility (high density, weak interactions) Si-MOS samples [54]. In contrast, for high-mobility (lower densities, strongly interacting regime) structures, as Fig. 10 shows, with temperature *increasing* $a_\sigma(T)$ crosses over from the conventional ballistic-type $-(B^2/T)$ to the unanomalous $-(B^2/T^2)$ dependence. Despite the absence of overheating of electrons [60], the diffusion regime of MC in the high mobility structures is not observed down to $T = 0.3 \text{ K}$.

One can see from Fig. 10, that the ballistic-type behavior $\propto T^{-1}$ extends up to temperatures 1.5-2 K (which are

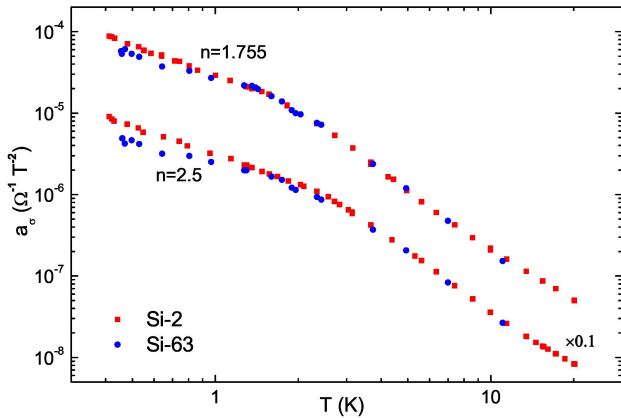


FIG. 10. Comparison of the temperature dependences of the prefactors $a_\sigma(T)$ for two samples Si2 and Si-63, and for two density values (in units of 10^{11}cm^{-2}). For clarity, the curves are scaled by the factors shown next to each curve.

a factor of 10 higher than the estimated diffusive/ballistic border $T_{\text{db}} \approx 0.2\text{K}$ [54], then it sharply changes to the novel dependence, $a_\sigma(T) \propto T^{-2}$, making the overall picture clearly inconsistent with theory predictions, Eq. (9). The crossover in Fig. 10 occurs rather sharply, as a kink on the double-log scale. The kink and the overall type of behavior were observed in the wide range of densities and were qualitatively similar for several studied high mobility samples. The next section shows that the observed effect in the in-plane magnetic field is associated with the onset of the two-phase state.

2. Phase separation effects in oscillatory magnetotransport

Measurements of the oscillatory magnetoresistance in high mobility Si-MOS structures in weak perpendicular magnetic fields were performed in Ref. [59]. It was found that the quantum oscillations in 2D electron systems are observed *down to the critical carrier density* n_c of the transition to strongly localized state. For such low densities, the oscillations exhibit an anticipated period, phase, and amplitude, even though the conductivity becomes essentially less than e^2/h , and, hence, the mean free path becomes less than the Fermi wavelength λ_F . It was concluded that this apparent contradiction with the Ioffe - Regel criterion for diffusive transport is caused by the emergence of an inhomogeneous state of the 2D system, in which the regions of diffusive and hopping conduction are spatially separated.

The existence of quantum resistivity oscillations down to the critical electron density provides an evidence for emerging inhomogeneity of the 2D system. As density approaches n_c , the “global” resistivity, calculated under assumption of a uniform current flow, becomes much greater than the “local” resistivity of the spatial areas, which contribute primarily to the oscillations amplitude.

This observation supports earlier conjecture of emergent inhomogeneity of the conductive regions near n_c [54] deduced from the analysis of magnetoconductivity in weak parallel fields. Thus, we associate the observed oscillations with Shubnikov-de Haas (SdH) effect within certain regions of the 2D space, in which the momentum relaxation times τ_p are much longer than that calculated from the global resistivity under assumption of the uniform current flow.

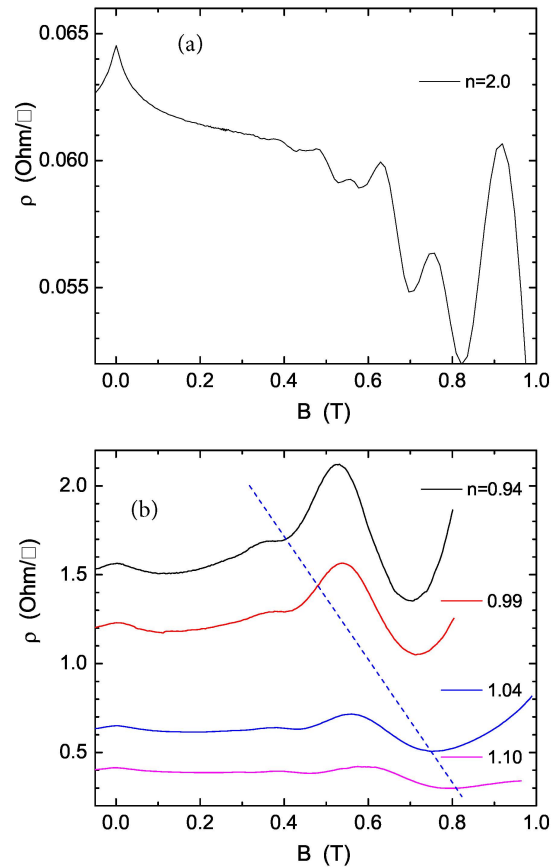


FIG. 11. Examples of quantum oscillations of the resistivity for (a) $n = 2 \times 10^{11}\text{cm}^{-2}$, and (b) 0.94, 1.00, and $1.04 \times 10^{11}/\text{cm}^2$. Dashed lines in panel (b) depict the upper boundary of analyzed magnetic fields. $T = 0.1\text{K}$. Adapted from [59].

In Ref. [53] it was shown that the correlated 2D electron system can be inhomogeneous even *at high electron densities*: it contains inclusions of collective localized (insulating) states (called “spin droplets”) in a conductive Fermi liquid. From the low density oscillatory transport measurements [59] the latter picture (we call it “bi-colored”) is supplemented with the data showing that the system is, in fact, “three-colored”. The conductive Fermi-liquid phase is not spatially homogeneous. Instead, it forms a pattern of regions with a large momentum relaxation time τ_p . These highly conductive regions are connected with each other through poorly conductive regions of Fermi liquid with lower τ_p -values.

3. Phase separation effects in zero field transport

Below we analyze the $\rho(T)$ and $\sigma(T)$ dependencies at zero field. The variations of these quantities in the relevant temperature range (see Fig. 12) for high mobility Si-MOS samples are large (up to a factor of 10), making the IC theory inapplicable.

Each $\rho(T)$ curve has two remarkable points: $\rho(T)$ maximum, T_{\max} , and inflection, T_{infl} [61, 62]. Whereas T_{\max} is an order of the renormalized Fermi energy, the inflection point happens at much lower temperatures, in the degenerate regime. Importantly, the inflection temperature appears to be close to the kink temperature (see Figs. 9, 12). Besides that, $T^*(n)$ is much higher than the ‘‘incoherence’’ temperature at which the phase coherence is lost (defined as $\tau_{\varphi}(T) = \tau$ [63]). This confirms that the kink, inflection and $\partial\chi/\partial n$ sign change are irrelevant to the single-particle interference effects [63–66].

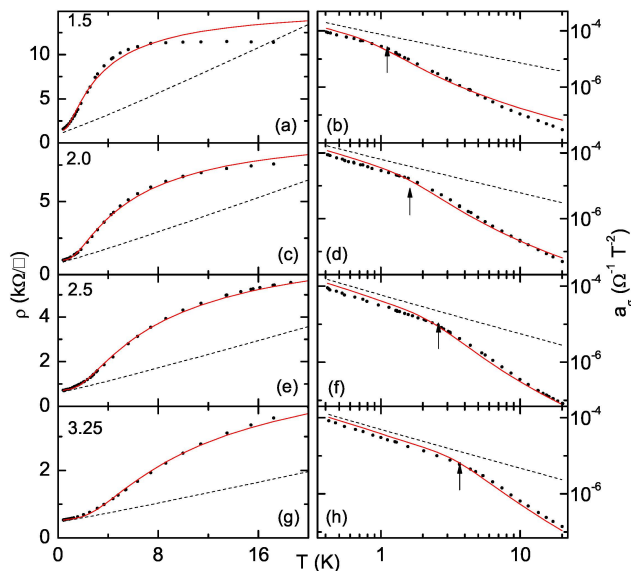


FIG. 12. Fitting $\rho(T, B = 0)$ dependencies (left) and $a_{\sigma}(T)$ (right) with the same set of the fitting parameters. Carrier densities (from top to bottom) are $n = 1.5, 2.0, 2.5,$ and $3.25 \times 10^{11} \text{cm}^{-2}$. Vertical arrows point at the kink positions. Adapted from [54].

One can see from Fig. 12 that the $\rho(T)$ temperature dependence is monotonic up to $T = T_F$, and follows one and the same additive resistivity functional form over a wide density range:

$$\begin{aligned} \rho(T) &= \rho_0 + \rho_1 \exp(-\Delta(n)/T), \\ \Delta(n) &= \alpha(n - n_c(B)), \end{aligned} \quad (10)$$

where $\rho_1(n, B)$ is a slowly decaying function of n , and $\rho_0(n, T)$ includes Drude resistivity and quantum corrections, both from the single-particle interference and interaction. Although the above empirical resistivity form has been suggested in Ref. [67] on a different footing, it fits well the $\rho(T)$ dependence for a number of material systems [67–74].

This empirical additive $\rho(T)$ form satisfies general requirements for the transport behavior in the vicinity of a critical point [62, 75]. This form implies two channel scattering and therefore agrees with the two-phase state of the low density 2D electronic system (cf. Matthiessen’s rule).

As noted above, $\rho(T)$ (and $\sigma(T)$) variations of the experimental data (Fig. 12) are so large, that the first order in T corrections, of course, cannot describe them. The simplest functional dependence, Eq. (10), correctly describes the inflection in $\rho(T)$ and the linear density dependence of the inflection temperature [67, 76]. Obviously, in this model $T_{\text{infl}} = \Delta/2$. To take magnetic field into account, and following the results of Ref. [76] we include to (Δ/T) all even in B and the lowest order in B/T terms, as follows:

$$\Delta(T, B, n)/T = \Delta_0(n)/T - \beta(n)B^2/T - \xi(n)B^2/T^2, \quad (11)$$

with $\Delta_0 = \alpha[n - n_c(0)]$.

Equations (10) and (11) link the magnetoconductance with the zero-field $\rho(T)$ temperature dependence. Combining equations (10) and (11), we obtain the $\rho(T, B)$ dependence as follows:

$$\begin{aligned} \rho(B, T) &= [\sigma_D - \delta\sigma \cdot \exp(-T/T_B)]^{-1} \\ &+ \rho_1 \exp\left(-\alpha \frac{n - n_c(0)}{T} - \beta \frac{B^2}{T} - \xi \frac{B^2}{T^2}\right) \end{aligned} \quad (12)$$

The term in the square brackets includes the Drude conductivity and interaction quantum corrections [55, 58], which are smoothly cut-off above $T = T_B \approx \Delta/2$. $\delta\sigma(T)$ was calculated in Ref. [54] using experimentally determined Fermi-liquid coupling constants $F_0^{\sigma}(n)$ [66, 77], and σ_D found by a conventional procedure [78].

From Eq. (12), the prefactor $a_{\sigma} = -(1/2)\partial^2\sigma/\partial B^2$ is calculated straightforward and in Fig. 12 is compared with experimental data. In the $\rho(T)$ fitting [Figs. 12 (a,c,e,g)], basically, there is only one adjustable parameter, $\rho_1(n)$, for each density. Indeed, $n_c(0)$ is determined from the conventional scaling analysis at $B = 0$ [62], and the slope $\alpha = 2\partial T_{\text{infl}}(n)/\partial n$ may be determined from Fig. 9.

One can see that both $\rho(T)$ and $a_{\sigma}(T)$ are well fitted; the model captures correctly the major data features, the steep $\rho(T)$ rise (including the inflection), and the kink in $a_{\sigma}(T)$ dependence. Within this model, the kink signifies a transition from the low-temperature magnetoconductance regime (where the interactions driven linear $\sigma(T)$ temperature dependence dominates and the exponential term may be neglected) to the high temperature regime governed by the steep exponential $\rho(T)$ rise.

We emphasize that both regimes are not related to the diffusive regime of interactions. This conclusion casts doubt on early attempts to use the two-parameter scaling for describing the magnetoresistance $\sigma(B)$ and the temperature dependence $\rho(T)$ within the renormalization group approach.

Thus, within the framework of a phenomenological two-phase model with two scattering channels, it is pos-

sible to explain all the observed features in transport and magnetotransport in a parallel field. It is important that their characteristic temperatures are close to the crossover temperature $T_{dM/dn}(n)$, where the spin magnetization per electron changes the sign [53] (see the insert in Fig. 9). Physically, this means that at temperatures below $T_{dM/dn}(n)$, collective droplets with a large spin (minority phase) “melt” with increasing density. In other words, the electrons added to the Fermi liquid improve screening thereby promoting the disappearance of spin droplets. At temperatures above $T_{dM/dn}(n)$, on the contrary, the number of spin droplets increases with increasing density; in this case, the electrons added to the 2D system prefer to combine and form new spin droplets. In Ref. [54], it was concluded that T^* may be related to the averaged energy spectrum of the SD phase.

C. Phase separation effect in spin susceptibility

Using a vector magnetic field technique with two independent superconducting coils, in Ref. [50] SdH oscillations were precisely measured and analyzed in various in-plane fields. Earlier [77, 79, 80], the oscillatory component $\delta\rho_{xx}$ was shown to be well fitted with conventional Lifshits-Kosevich formula [79–82]; this enables accurate extraction of the spin susceptibility χ^* and density of mobile carriers n_{SdH} from the beating of oscillations. In particular, χ^* values have been determined with an accuracy of $\sim (1 - 2)\%$ as a function of the in-plane field.

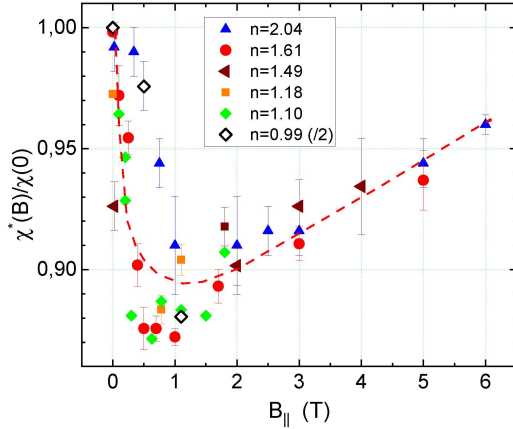


FIG. 13. Summary of $\chi^*(B_{\parallel})/\chi^*(0)$ data versus B_{\parallel} for two samples and for several densities. For the lowest density $n = 0.99$, the $\chi^*(B_{\parallel})/\chi^*(0)$ variations are scaled down by 2 times. The density is indicated in units of 10^{11}cm^{-2} , $T = 0.1\text{K}$. Adapted from Ref. [50]

Figure 13 shows the main result of [50] - a sharp non-monotonic dependence of χ^* on the in-plane field. The characteristic $\delta\chi^*(B)/\chi^*(0)$ variations are in the range from $\sim 25\%$ at low densities to $\sim 6\%$ at high densities $10 \times 10^{11}\text{cm}^{-2}$. The data reported in [50] coincide in

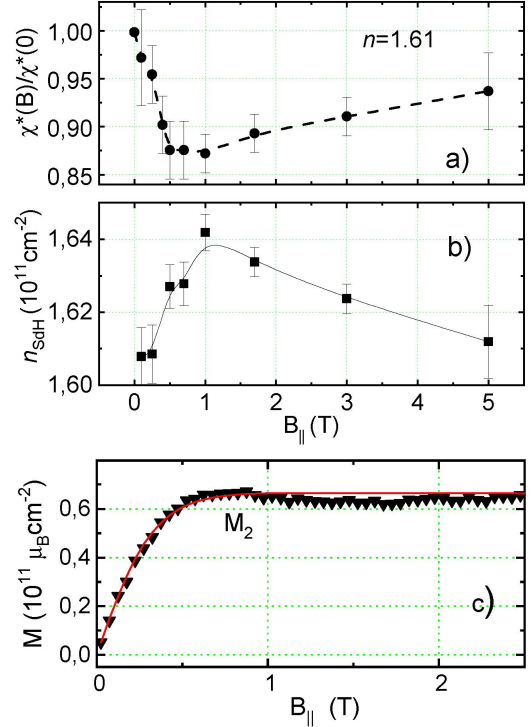


FIG. 14. Correlation between the in-plane field dependence of (a) $\chi^*(B)/\chi^*(0)$, and (b) density $n_{\text{SdH}}(B)$. Red curve shows $\tanh(\mu_B B/k_B T)$ -fitting of the experimental $M(B)$ data. The zero-field densities are $n_0 = 1.61 \times 10^{11}\text{cm}^{-2}$ for (a) and (b), and $1.4 \times 10^{11}\text{cm}^{-2}$ for (c). Temperature $T = 0.1\text{K}$. Adapted from Ref. [50].

the $B_{\parallel} \rightarrow 0$ limit with the $\chi^*(B = 0)$ values reported Refs. [66, 77]. The characteristic field of the $\chi^*(B)$ -minimum, $B_{\parallel} \sim 1\text{T}$ for $n = (1.1 - 2) \times 10^{11}\text{cm}^{-2}$, is much weaker than the field of complete spin polarization of the 2D system $B_p \sim 20\text{T}$. Evidently, in a homogeneous single-phase Fermi liquid the only characteristic field is B_p .

The spin susceptibility variations $\delta\chi^*(B)$ measured from SdH oscillations are relevant to the mobile carriers. The $\delta\chi^*(B)$ data also appears to correlate (i) with variation of the mobile carrier density δn_{SdH} (see Fig. 14), and (ii) with thermodynamic magnetization $\partial M/\partial n$ of the collective localized states $M(B)$ (see Fig. 8) [53]. This correlation prompts that the observed changes in the properties of extended states are caused by the changes in magnetization of the localized states and by the subsequent redistribution of carriers between the two subsystems. The range of accessible densities where δn_{SdH} could be measured is limited from low densities side, on the verge of the transition to fully localized state. Here the $n_{\text{SdH}}(B)$ variation cannot be measured precisely and variations of $\chi^*(B)$ cannot be traced to higher field, because application of an in-plane field quickly causes localization of the 2D system [83–86]

From the density redistribution at ultralow tempera-

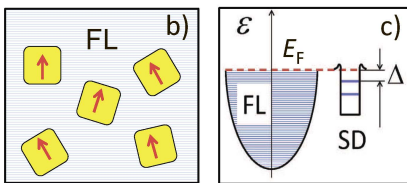


FIG. 15. (a) Schematic spatial arrangement of the two-phase state and (b) the energy band diagram of the two-phase system.

ture it follows that energy of the localized states is located in the close vicinity of the Fermi energy, in order to allow for the carrier exchange at ultralow temperatures between two electronic subsystems. No temperature dependence of δn_{SdH} was observed within the range 0.1–0.5 K, hence, the carrier redistribution occurs elastically, via tunneling. The energy diagram describing schematically the two-phase state is shown in Fig. 15. Note, that this picture is essentially different from the conventional model of the disorder-localized single-particle states in the tail of the conduction band [8, 87, 88].

It is worthnoting that the Fermi-liquid density deduced from SdH oscillations in the phase-separated system is determined by the local density in the Fermi-liquid “lakes” (where the carriers possess the highest relaxation time), rather than by the total or by average density; this picture holds until the delocalized states (Fermi-liquid lakes) percolate. The carrier redistribution between two phases in the 2D system is not easy to determine by other techniques. For example, the capacitance measurements taken at frequencies $10^1 - 10^5$ Hz (1 nF, 10 kOhm/□) probe the total charge density that includes both SD and mobile states. In order to separate the SD and FL states, the capacitance measurements should be done at frequency of $10^{10} - 10^{12}$ Hz, inaccessible for the gated structure. Hall measurements cannot also shed a light on the density distribution of the delocalized and SD states, because Hall voltage becomes irrelevant to the carrier density in the vicinity of the localization transition [89].

Measurements [50] have been performed with a gated Si-MOS structure at a fixed gate voltage V_g , whereas B_{\parallel} and T varied. Under this condition the total charge is conserved. Therefore, a change in the mobile carrier density (δn_{SdH}) in the FL-regions can only occur via carriers transfer to the localized regions (SD) and back [42, 53].

To describe the data, a simple thermodynamic model with two phases coexisting in equilibrium has been applied in Ref. [50]. The model was found is capable to explain the results qualitatively, and even quantitatively, with some parameters determined in experiments. In particular, the $n_{\text{FL}}(B)$ dependence calculated within this model for a representative density $1.4 \times 10^{11} \text{ cm}^{-2}$ is shown in Fig. 16. It is rather similar to the direct experimental data of Fig. 14b; the similarity supports the validity of the two-phase thermodynamic approach.

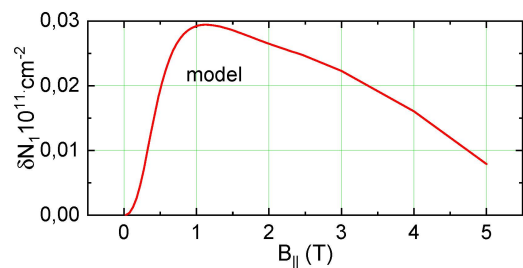


FIG. 16. Model curve $\delta N_1(B_{\parallel})$ calculated from experimental data as described in the text. Adapted from Ref. [50].

Summarizing the content of this section, we conclude that the results of [50, 54] give reason to believe that the phase separation in a correlated 2D electron system exists not only near the transition to the insulator state (as was revealed in local compressibility measurements [30]), but also in a wide range of densities, even deep in the “metallic regime” of high conductivity $\sigma = (3 - 80) \times (e^2/h)$ [90].

V. CONCLUSIONS

A two-dimensional electron system in silicon structures for the last 50 years has served as a research platform, where many new exciting effects have been discovered, including the integer quantum Hall effect, negative electron compressibility, strong renormalization of electron effective mass and spin susceptibility, etc. This 2DE system is strongly correlated in a wide range of densities, where the energy of interparticle interactions is much greater than the kinetic Fermi energy.

Local compressibility measurements [30] evidenced the emergence of an inhomogeneous state on a microscopic scale in 2D system with a decrease in the concentration of carriers near the transition to the insulator state. For a long time, this result was not appreciated when considering a macroscopic system with high conductivity as, on average, a homogeneous Fermi liquid. Within such approach, the averaged values of the Fermi-liquid parameters were experimentally determined and the averaged properties in charge transport were quantitatively described. However, later thermodynamic measurements [53] revealed signatures of the coexistence in thermodynamic equilibrium, in a wide range of densities, of the majority Fermi liquid and the minority phase of collective localized states with large spin.

Subsequent precision measurements of SdH oscillations in the presence of an in-plane field revealed a sharp change in the spin susceptibility $\chi^*(B_{\parallel})$ and a simultaneous change in the concentration of mobile carriers $\delta n_{\text{SdH}}(B)$ in correlated 2D electron system. The two effects correlate well with each other and with the thermodynamic magnetization of the localized SD states. It is found that the origin of these variations is the mag-

netization of collective localized states (“spin droplets”) and, as a result, the redistribution of carriers between the two phases. Independent measurements of spin magnetization and magnetoresistance in a weak in-plane field, as well as the temperature dependence of resistance, revealed the existence of a new energy scale $T^*(n) \ll T_F$, which marks a crossover between the regime of predominant proliferation of the SD states and the regime of their disappearance. The results of the considered experiments were described within the framework of a phenomenological two-phase model. These results and their successful description with two-phase model provide the solid evidence for the phase separation in the interacting 2D electron system even at relatively high carrier densities, deeply in the “metallic” regime of high conductivity $\sigma = (3 - 80) \times (e^2/h)$ [90]. The latter regime was commonly considered as a pure Fermi liquid.

In quasi-one-dimensional systems, the main driving force of the phase separation is associated with the nesting of the Fermi surface, which leads to the appearance of a spin or charge density wave coexisting with a paramagnetic or superconducting metallic phase in the vicinity of the phase transition [4, 91, 92]. In 2D systems, instability can also occur in the charge or spin exchange channel. An interesting and still debatable issue is the microscopic mechanism behind the electronic phase separation that is experimentally observed in correlated low dimensional electron systems.

Several scenarios were theoretically considered, where in the majority Fermi liquid the minority phases such as Wigner solid “droplets”, or spin polarized “droplets” emerge due to the local Wigner crystallization [93, 94], local Stoner instability [95–101], or, alternatively, the topology of the Fermi surface changes [102–106].

The experimental results presented in this review evidence for the existence of spin-polarized droplets as the minority phase in the majority Fermi liquid sea. It is possible, however, that with a stronger interaction or a weaker disorder, instability in the charge channel may also manifest itself.

Attempts to ignore the tendency to spin/charge instability or instability of the Fermi surface, considering only the semiclassical effects of disorder and screening [107], although they are able to describe some experimental results (such as negative compressibility, transport in the zero field), but give an overly simplified picture of the phenomenon of phase separation and miss the structure of the heterophase state.

The microscopic mechanism responsible for the phase separation, for the redistribution of carriers between two phases, as well as the energy structure of the minority phase remain interesting and still open issues.

VI. ACKNOWLEDGEMENTS

The author is grateful to B. Altshuler, G. Bauer, G. Brunthaler, I.S. Burmistrov, M. D’Iorio, J. Campbell, V.S. Edel’man, M.E. Gershenson, N. Klimov, H. Kojima, S. V. Kravchenko, A. Yu. Kuntsevich, D. L. Maslov, L. A. Morgun, O. Prus, M. Reznikov, D. Rinberg, S. G. Semenchinsky, and N. Tench for fruitful collaboration in developing experimental methods, performing measurements, discussing the results, and writing the original papers. Financial support from the State assignment of the research at P.N. Lebedev Physical Institute (Grant # 0019-2019-0006) and from Russian Foundation for Basic research (#18-02-01013) is acknowledged.

-
- [1] T. V. Ramakrishnan, H. R. Krishnamurthy, S. R. Hassan, G. V. Pai, *Theory of Insulator Metal Transition and Colossal Magnetoresistance in Doped Manganites*, Phys. Rev. Lett. **92**, 157203 (2004).
 - [2] A.A. Gorbatsevich, Yu.V. Kopaev, and I.V. Tokatly, *Phase separation and dielectric correlations in HTSC*, Physica C **223**, 95 (1994).
 - [3] V. Z. Kresin, S. G. Ovchinnikov, S. A. Wolf, *Superconducting state*, (Oxford University Press, UK, 2021).
 - [4] *The Physics of Organic Superconductors and Conductors*, ed. by A. G. Lebed (Springer-Verlag, Berlin-Heidelberg-New York-Tokyo, 2008). ISBN 978-3-540-76667-4
 - [5] Eduardo Fradkin, Steven A. Kivelson, Michael J. Lawler, James P. Eisenstein, Andrew P. Mackenzie. *Nematic Fermi Fluids in Condensed Matter Physics* Annu. Rev. Condens. Matter Phys. **1**, 153-178 (2010)
 - [6] M.Yu. Kagan, K.I. Kugel, A.L. Rakhmanov *Electronic phase separation: Recent progress in the old problem*, Physics Reports **916**, 1 (2021).
 - [7] G. Giuliani and G. Vignale, *Quantum Theory of the Electron Liquid* (Cambridge University Press, Cambridge, 2005).
 - [8] T. Ando, A.B. Fowler, and F. Stern, *Electronic properties of two-dimensional systems* Rev. Mod. Phys. **54**, 437 (1982).
 - [9] M. S. Bello, E. I. Levin, B. I. Shklovskii, and A. L. Efros, *Density of localized states in the surface impurity band of a metal-insulator-semiconductor structure*, Sov. Phys. JETP **53**, 822 (1981); [Zh. Exp. Teor. Fiz. **80**, 1596 (1983)].
 - [10] A. L. Efros, *Density of states of 2D electron gas and width of the plateau of IQHE*, Solid State Commun. **65**, 1281 (1988).
 - [11] S. V. Kravchenko, V. M. Pudalov, S. G. Semenchinsky, *Negative density of states if 2D electrons in a strong magnetic field*, Phys. Lett. A **141**, 71 (1989).
 - [12] S. V. Kravchenko, V. M. Pudalov, D. A. Rinberg, and S. G. Semenchinsky, *Direct observation of the influence of electron-electron interaction on the chemical potential of the 2D electron gas*, Phys. Lett. A **146**, 535 (1990).
 - [13] S. V. Kravchenko, D. A. Rinberg, S. G. Semenchinsky, and V. M. Pudalov, *Evidence for the influence of electron-electron interaction on the chemical potential of*

- the two-dimensional electron gas*, Phys. Rev. B **42**, 3741 (1990).
- [14] J. P. Eisenstein, L. N. Pfeiffer, and K. W. West, *Negative compressibility of interacting two-dimensional electron and quasiparticle gases*, Phys. Rev. Lett. **68**, 674 (1992).
- [15] J. P. Eisenstein, L. N. Pfeiffer, and K. W. West, *Compressibility of the two-dimensional electron gas: Measurements of the zero-field exchange energy and fractional quantum Hall gap*, Phys. Rev. B **50**, 1760 (1994).
- [16] S. Shapira U. Sivan, P. M. Solomon, E. Buchstab, M. Tischler, and G. Ben Yoseph, *Thermodynamics of a Charged Fermion Layer at High r_s Values*, Phys. Rev. Lett. **77**, 3181 (1996).
- [17] V. A. Gergel' and R. A. Suris, *Fluctuations of the surface potential*, JETP **48**, 95 (1978)
- [18] A. M. Finkelstein, *The influence of Coulomb interaction on the properties of disordered metals*, Sov. Phys. JETP **57**, 97 (1983); [Zh. Eksp. Teor. Fiz. **84**, 168 (1983)].
- [19] A. M. Finkelstein, *Weak localization and coulomb interaction in disordered systems*, Z. Phys. **56**, 189 (1984).
- [20] C. Castellani, C. Di Castro, P. A. Lee, and M. Ma, *Interaction-driven metal-insulator transitions in disordered fermion systems*, Phys. Rev. B **30**, 527 (1984).
- [21] C. Castellani, C. di Castro, P. A. Lee, M. Ma, S. Sorella, and E. Tabet, *Spin fluctuations in disordered interacting electrons*, Phys. Rev. B **30**, 1596 (1984).
- [22] B. L. Altshuler and A. G. Aronov, in *Electron-Electron Interactions in Disordered Systems*, ed. by A. L. Efros and M. Pollak (Elsevier Science Publishers, New York, 1985).
- [23] D. Belitz and T. R. Kirkpatrick, *The Anderson-Mott transition*, Rev. Mod. Phys. **66**, 261 (1994).
- [24] Q. Si and C. M. Varma, *Metal-Insulator Transition of Disordered Interacting Electrons*, Phys. Rev. Lett. **81**, 4951 (1998).
- [25] A. A. Pastor and V. Dobrosavljevic, *Melting of the Electron Glass*, Phys. Rev. Lett. **83**, 4642 (1999).
- [26] B. Tanatar and D. M. Ceperley, *Ground state of the two-dimensional electron gas*, Phys. Rev. B **39**, 5005 (1989).
- [27] S. Orozco, R. M. Mendez-Moreno, and M. Moreno, *Compressibility of a two-dimensional electron gas*, Phys. Rev. B **67**, 195109 (2003).
- [28] Asgari, R., and B. Tanatar, *Effects of disorder on the ground-state energy of a two-dimensional electron gas*, Phys. Rev. B, **65**, 085311 (2002).
- [29] S. C. Dultz and H. W. Jiang, *Thermodynamic Signature of a Two-Dimensional Metal-Insulator Transition*, Phys. Rev. Lett. **84**, 4689 (2000).
- [30] S. Ilani, A. Yacoby, D. Mahalu, and H. Shtrikman, *Unexpected Behavior of the Local Compressibility near the Metal-Insulator Transition*, Phys. Rev. Lett. **84**, 3133 (2000).
- [31] S. Ilani, A. Yacoby, D. Mahalu, and H. Shtrikman, *Microscopic Structure of the Metal-Insulator Transition in Two Dimensions*, Science **292**, 1354 (2001).
- [32] G. Allison, E. A. Galaktionov, A. K. Savchenko, S. S. Safonov, M. M. Fogler, M. Y. Simmons, and D. A. Ritchie, *Thermodynamic Density of States of Two-Dimensional GaAs Systems near the Apparent Metal-Insulator Transition*, Phys. Rev. Lett. **96**, 216407 (2006).
- [33] Junren Shi and X. C. Xie, *Droplet State and the Compressibility Anomaly in Dilute 2D Electron Systems*, Phys. Rev. Lett. **88**, 086401 (2002).
- [34] M. M. Fogler, *Nonlinear screening and percolative transition in a two-dimensional electron liquid*, Phys. Rev. B **69**, 121409 (R) (2004).
- [35] R. K. Goodall, R. J. Higgins, and J. P. Harrang, *Capacitance measurements of a quantized two-dimensional electron gas in the regime of the quantum Hall effect*, Phys. Rev. B **31**, 6597 (1985).
- [36] S. V. Kravchenko, J. M. Caulfield, J. Singleton, H. Nielsen, V. M. Pudalov, *Electron-Electron Interaction in the 2D Electron Gas in Silicon*, Phys. Rev. B **47**, 12961 (1993).
- [37] T. P. Smith, W. I. Wang, and P. J. Stiles, *Two-dimensional density of states in the extreme quantum limit*, Phys. Rev. B **34**, 2995 (1986).
- [38] T. P. Smith, B. B. Goldberg, P. J. Stiles, M. Heiblum, *Direct measurement of the density of states of a two-dimensional electron gas*, Phys. Rev. B **32**, 2696 (1985).
- [39] V. Mosser, D. Weiss, K. v. Klitzing, K. Ploog, G. Weinmann, *Density of states of GaAs-AlGaAs-heterostructures deduced from temperature dependent magnetocapacitance measurements*, Sol. St. Commun. **58**, 5 (1986).
- [40] H. Nielsen, S. V. Kravchenko, D. A. Rinberg, V. M. Pudalov, *On the Negative Dielectric Permittivity in the Quantum Hall Effect Regime*, Physica B **184**, 323 issue 1-4, (1993).
- [41] Y. Tupikov, A. Yu. Kuntsevich, V. M. Pudalov, I. S. Burmistrov, *Temperature derivative of the chemical potential and its magnetooscillations in two-dimensional system*, JETP Lett. **101**, 125 (2015).
- [42] A. Yu. Kuntsevich, Y. V. Tupikov, V. M. Pudalov, and I. S. Burmistrov, *Strongly Correlated Two-dimensional Plasma Explored from Entropy Measurements*, Nature Commun. **6**, 7298 (2015).
- [43] V. M. Pudalov, S. G. Semenchinsky, V. S. Edelman, *Hysteresis Phenomena in Charging of Si MOSFET in Quantizing Magnetic Field*, Sol. State Commun. **51**, 713 (1984).
- [44] V. M. Pudalov, S. G. Semenchinskii, V.S. Edel'man, *Oscillations of the chemical potential and the energy spectrum of electrons in the inversion layer at a silicon surface in a magnetic field* JETP **62**, 1079 (1985).
- [45] V. M. Pudalov, S. G. Semenchinskii, *Quantum oscillations of the density and Fermi energy of electrons at an inversion layer in magnetic field*, JETP Lett. **44**, 677 (1986).
- [46] V. M. Pudalov, *Measurements of the magnetic properties of conduction electrons*, Physics - Uspekhi **64**, 3 (2021).
- [47] S. Chakravarty, S. Kivelson, C. Nayak, and K. Voelker, *Wigner glass, spin liquids and the metal-insulator transition*, Philos. Mag. B **79**, 859 (1999).
- [48] L. P. Kouwenhoven et al., in *Mesoscopic Electron Transport*, ed. by L. L. Sohn, L. P. Kouwenhoven, and G. Schon, NATO ASI Series (Kluwer Academic Publishers, Dordrecht, 1996).
- [49] B. L. Altshuler and D. L. Maslov, *Theory of Metal-Insulator Transitions in Gated Semiconductors*, Phys. Rev. Lett. **82**, 145 (1999).
- [50] V. M. Pudalov, and M. E. Gershenson, *Magnetic field driven redistribution between extended and localized electronic states in high-mobility Si MOSFETs at low temperatures*, Phys. Rev. B **104**, 035407 (2021).

- [51] O. Prus, Y. Yaish, M. Reznikov, U. Sivan, and V. Pudalov, *Thermodynamic spin magnetization of strongly correlated two-dimensional electrons in a silicon inversion layer*, Phys. Rev. B **67**, 205407 (2003).
- [52] M. Reznikov, A. Yu. Kuntsevich, N. Teneh, V. M. Pudalov, *Thermodynamic magnetization of two-dimensional electron gas measured over wide range of densities*, JETP Lett. **92**, 470 (2010).
- [53] N. Teneh, A. Yu. Kuntsevich, V. M. Pudalov, and M. Reznikov, *Spin-Droplet State of an Interacting 2D Electron System*, Phys. Rev. Lett. **109**, 226403 (2012).
- [54] L. A. Morgun, A. Yu. Kuntsevich, and V. M. Pudalov, *Novel energy scale in the interacting two-dimensional electron system evidenced from transport and thermodynamic measurements*, Phys. Rev. B **93** 235145 (2016).
- [55] G. Zala, B. N. Narozhny, I. L. Aleiner, *Interaction corrections at intermediate temperatures: Magnetoresistance in a parallel field*, Phys. Rev. B **65**, 020201 (2001).
- [56] A. Gold, V. T. Dolgoplov, *Temperature dependence of the conductivity for the two-dimensional electron gas: Analytical results for low temperatures*, Phys. Rev. B **33**, 1076 (1986).
- [57] V. T. Dolgoplov, A. V. Gold, *Magnetoresistance of a two-dimensional electron gas in a parallel magnetic field*, JETP Lett. **71**, 27 (2000).
- [58] G. Zala, B. N. Narozhny, I. L. Aleiner, *Interaction corrections at intermediate temperatures: Longitudinal conductivity and kinetic equation*, Phys. Rev. B **64**, 214204 (2001).
- [59] V. M. Pudalov, and M. E. Gershenson, *Experimental evidence for an inhomogeneous state of the correlated two-dimensional electron system in the vicinity of a metal-insulator transition*, JETP Letters **111**, 225 (2020).
- [60] O. Prus, M. Reznikov, U. Sivan, V.M.Pudalov, *Cooling of electrons in a silicon inversion layer*, Phys. Rev. Lett. **88**, 016801 (2002).
- [61] D. A. Knyazev, O. E. Omel'yanovskii, V. M. Pudalov, and I. S. Burmistrov, *Critical Behavior of Transport and Magnetotransport in a 2D Electron System in Si near the Metal-Insulator*, JETP Lett. **84**, 662 (2006).
- [62] D. A. Knyazev, O. E. Omel'yanovskii, V. M. Pudalov, and I. S. Burmistrov, *Metal-Insulator Transition in Two Dimensions: Experimental Test of the Two-Parameter Scaling*, Phys. Rev. Lett. **100**, 046405 (2008).
- [63] G. Brunthaler, A. Prinz, G. Bauer, and V. M. Pudalov, *Exclusion of Quantum Coherence as the Origin of the 2D Metallic State in High-Mobility Silicon Inversion Layers*, Phys. Rev. Lett. **87**, 096802 (2001).
- [64] V. M. Pudalov, G. Brunthaler, A. Prinz, G. Bauer, *Logarithmic temperature dependence of the conductivity of the two-dimensional metal*, JETP Lett. **68**, 534 (1998).
- [65] V.M. Pudalov, G. Brunthaler, A. Prinz, G. Bauer, *Metal-insulator transition in two dimensions*, Physica E **3**, 79 (1998).
- [66] N. N. Klimov, D. A. Knyazev, O. E. Omel'yanovskii, V. M. Pudalov, H. Kojima, and M. E. Gershenson, *Interaction effects in conductivity of a two-valley electron system in high-mobility Si inversion layers*, Phys. Rev. B **78**, 195308 (2008).
- [67] V. M. Pudalov, *Unconventional metallic state in two-dimensional system with broken inversion symmetry*, JETP Lett. **66**, 175 (1997).
- [68] Y. Hanein, U. Meirav, D. Shahar, C. C. Li, D. C. Tsui, H. Shtrikman, *The Metalliclike Conductivity of a Two-Dimensional Hole System*, Phys. Rev. Lett. **80**, 1288 (1998).
- [69] S. J. Papadakis, M. Shayegan, *Apparent metallic behavior at $B = 0$ of a two-dimensional electron system in AIs* Phys. Rev. B **57**, R15068 (1998).
- [70] X. P. A. Gao, A. P. Mills Jr., A. P. Ramirez, L. N. Pfeiffer, K. W. West, *Two-Dimensional Metal in a Parallel Magnetic Field*, Phys. Rev. Lett. **88**, 166803 (2002).
- [71] T. Hörmann, G. Brunthaler, *Pronounced metal-insulator transition according to dipole trap model for two-dimensional Si-MOS structures*, Physica E **40**, 1235 (2008).
- [72] J. Y. Zhang, C. A. Jackson, Ru Chen, S. Raghavan, P. Moetakef, L. Balents, and S. Stemmer, *Correlation between metal-insulator transitions and structural distortions in high-electron-density SrTiO₃ quantum wells*, Phys. Rev. B **89**, 075140 (2014).
- [73] S. Raghavan, J. Y. Zhang, S. Stemmer, *Two-dimensional electron liquid at the (111) Sm-TiO₃/SrTiO₃ interface*, Appl. Phys. Lett. **106**, 132104 (2015).
- [74] P. Moetakef, C. A. Jackson, J. Hwang, L. Balents, S. J. Allen, S. Stemmer, *Toward an artificial Mott insulator: Correlations in confined high-density electron liquids in SrTiO₃*, Phys. Rev. B **86**, 201102(R) (2012).
- [75] B. L. Altshuler, D. L. Maslov, V. M. Pudalov, *Metal-Insulator Transition in 2D: Anderson Localization by temperature-dependent disorder?*, Phys. Stat.Sol.(b), **218**, 193 (2000)
- [76] V.M. Pudalov, G. Brunthaler, A. Prinz, G. Bauer, *Effect of the In-Plane Magnetic Field on Conduction of the Si-inversion Layer: Magnetic Field Driven Disorder*, arXiv:cond-mat/0103087 (2001).
- [77] V. M. Pudalov, M. E. Gershenson, H. Kojima, N. Butch, E. M. Dizhur, G. Brunthaler, A. Prinz, and G. Bauer, *Low-Density Spin Susceptibility and Effective Mass of Mobile Electrons in Si Inversion Layers*, Phys. Rev. Lett. **88**, 196404 (2002).
- [78] V. M. Pudalov, M. E. Gershenson, H. Kojima, G. Brunthaler, A. Prinz, G. Bauer, *Interaction Effects in Conductivity of Si Inversion Layers at Intermediate Temperatures*, Phys. Rev. Lett. **91**, 126403 (2003).
- [79] V. M. Pudalov, A. Yu. Kuntsevich, M. E. Gershenson, I. S. Burmistrov, and M. Reznikov, *Probing spin susceptibility of a correlated two-dimensional electron system by transport and magnetization measurements*, Phys. Rev. B **98**, 155109 (2018).
- [80] V. M. Pudalov, M. E. Gershenson, and H. Kojima, *Probing electron interactions in a two-dimensional system by quantum magneto-oscillations*, Phys. Rev. B **90**, 075147 (2014)
- [81] I. M. Lifshitz and A. M. Kosevich, *Sov. Phys. JETP* **6**, 67 (1958).
- [82] A. Isihara, L. Smrčka, *Density and magnetic field dependences of the conductivity of two-dimensional electron systems*, J. Phys. C: Solid State Phys. **19**, 6777 (1986).
- [83] D. Simonian, S. V. Kravchenko, M. P. Sarachik, and V.M.Pudalov, *Magnetic Field Suppression of the Conducting Phase in Two Dimensions*, Phys. Rev. Lett. **79**, 2304 (1997).
- [84] V. M. Pudalov, G. Brunthaler, A. Prinz, and G. Bauer, *Instability of the two-dimensional metallic phase to a parallel magnetic field*, JETP Lett. **65**, 932 (1997).

- [85] V.M. Pudalov, G. Brunthaler, A. Prinz, G. Bauer, *Breakdown of the anomalous two-dimensional metallic phase in a parallel magnetic field*, Physica B, **249-251**, 697 (1998)
- [86] S. V. Kravchenko, D. Simonian, M. P. Sarachik, A. D. Kent, V. M. Pudalov, *Effect of Tilted Magnetic Field on the Anomalous $H=0$ Conducting Phase in High-Mobility Si MOSFETs*, Phys. Rev. B, **58**, 3553 (1998).
- [87] S. A. Vitkalov, M. P. Sarachik, T. M. Klapwijk, *Spin polarization of strongly interacting two-dimensional electrons: The role of disorder*, Phys. Rev. B **65**, 201106(R) (2002).
- [88] A. Gold and V. T. Dolgoplov, *On the role of disorder in transport and magnetic properties of the two-dimensional electron gas*, J. Phys.: Condens. Matter **14**, 7091 (2002).
- [89] V. M. Pudalov, M. D'Iorio, J. Campbell, *Hall resistane and quantized Hall effect to insulator transitions in a 2D electron system*, JETP Lett. **57**, 608 (1993).
- [90] V. M. Pudalov, G. Brunthaler, A. Prinz, and G. Bauer, *Maximum metallic conductivity in Si-MOS structures*, Phys. Rev. B **60**, R2154 (1999).
- [91] A. V. Kornilov, V. M. Pudalov, Y. Kitaoka, K. Ishida, G.-q. Zheng, T. Mito, and J. S. Qualls, *Macroscopically Inhomogeneous State at the Border Between the Superconducting, Antiferromagnetic, and Metallic Phases in Quasi One-Dimensional (TMTSF) $_2$ PF $_6$* , Phys. Rev. B **69**, 224404 (2004).
- [92] Ya. A. Gerasimenko, S. V. Sanduleanu, V. A. Prudkoglyad, A. V. Kornilov, J. Yamada, J. S. Qualls, and V. M. Pudalov *Coexistence of superconductivity and spin-density wave in (TMTSF) $_2$ ClO $_4$: Spatial structure of the two-phase state*, Phys. Rev. B **89**, 054518 (2014).
- [93] B. Spivak, *Phase separation in the two-dimensional electron liquid in MOSFETs*, Phys. Rev. B **67**, 125205 (2003).
- [94] B. Spivak, and S. A. Kivelson, *Phases intermediate between a two-dimensional electron liquid and Wigner crystal*, Phys. Rev. B **70**, 155114 (2004).
- [95] C. Sloggett and O. P. Sushkov, *Electron correlations in two-dimensional small quantum dots*, Phys. Rev. B **71**, 235326 (2005).
- [96] Y. V. Stadnik and O. P. Sushkov, *Interacting spin droplets and magnetic properties of a low-density two-dimensional electron gas*, Phys. Rev. B **88**, 125402 (2013).
- [97] E. Eisenberg, R. Berkovits, *Disorder-induced spin polarization in restricted geometries*, Phys. Rev. B **60**, 15261 (1999).
- [98] I. L. Kurland, I. L. Aleiner, and B. L. Altshuler, *Mesoscopic magnetization fluctuations for metallic grains close to the Stoner instability*, Phys. Rev. B **62**, 14886 (2000).
- [99] B. N. Narozhny, I. L. Aleiner, A. I. Larkin, *Magnetic fluctuations in two-dimensional metals close to the Stoner instability*, Phys. Rev. B **62**, 14898 (2000).
- [100] G. Benenti, G. Caldara, D. L. Shepelyansky, *Spin-Polarized Ground State for Interacting Electrons in Two Dimensions*, Phys. Rev. Lett. **86**, 5333 (2001).
- [101] E. V. Repin, I. S. Burmistrov, *Inelastic electron scattering off a quantum dot in the cotunneling regime: The signature of mesoscopic Stoner instability*, Phys. Rev. B **93**, 165425 (2016).
- [102] V. A. Khodel, V. R. Shaginyan, *Superfluidity in system with fermion condensate*, JETP Lett. **51**, 553 (1990).
- [103] G. E. Volovik, *A new class of normal Fermi liquids*, JETP Lett. **53**, 222 (1991).
- [104] V. A. Khodel, J. W. Clark, and M. V. Zverev, *Topology of the Fermi surface beyond the quantum critical point*, Phys. Rev. B **78**, 075120 (2008).
- [105] V. T. Dolgoplov, M. Yu. Melnikov, A. A. Shashkin, S. V. Kravchenko, *Band Flattening and Landau Level Merging in Strongly-Correlated Two-Dimensional Electron Systems*, JETP Letters **116**, 156 (2022).
- [106] V. T. Dolgoplov, *Two-dimensional system of strongly interacting electrons in silicon (100) structures*, Phys. Usp., **62**, 633 (2019).
- [107] S. Das Sarma, E. H. Hwang, and Qiuzi Li, *Two-dimensional metal-insulator transition as a potential fluctuation driven semiclassical transport phenomenon*, Phys. Rev. B **88**, 155310 (2013).